

DOI: <http://dx.doi.org/10.21123/bsj.2022.6420>

Using Remote Sensing and Geographic Information Systems to Study the Change Detection in Temperature and Surface Area of Hamrin Lake

Ahmed Bahjat Khalaf 

Department of Soil and Water Resources (College of Agriculture, University of Diyala, Iraq
E-mails address: bahjatahmed098@gmail.com

Received 16/6/2021, Accepted 22/12/2021, Published Online First 20/3/2022, Published 1/10/2022



This work is licensed under a [Creative Commons Attribution 4.0 International License](https://creativecommons.org/licenses/by/4.0/).

Abstract:

This study was conducted on Lake Hamrin situated in Diyala governorate, focal Iraq, between latitudes $44^{\circ} 53' 26.16''$ - $45^{\circ} 07' 28.03''$ and $34^{\circ} 04' 24.75''$ - $34^{\circ} 19' 12.74''$. As in this study, the surface area of Hamrin Lake was calculated from satellite images during the period from October 2019 to September 2020, with an average satellite image for each month, furthermore, by utilizing the Normalized Differences Water Index (NDWI), the largest surface area was $264,617 \text{ km}^2$ for October and the lowest surface area 140.202 km^2 for September. The surface temperature of the lake water was also calculated from satellite images of the Landsat 8 satellite, based on bands 10 (Thermal Infrared 1) and 11 (Thermal Infrared 2) that are sensitive to thermal radiation, as the highest surface temperature reached in June 45.49°C degrees Celsius due to the high temperatures for this month and the lowest in February 3.09°C degrees Celsius, which is one of the months in which temperatures drop to the lowest level. The utilization of remote sensing and GIS innovations has helped a lot in checking changes, whether in surface area or temperature, which saves effort, time and cost. The results of this study put decision makers in taking the necessary precautions for the seasons of water scarcity and drought to meet the community's water needs in the areas of multiple human consumptions and at the same time take advantage of rainy seasons and water abundance to develop long-term strategic plans to maintain a sustainable water balance.

Keywords: Climate change, Land surface temperature, Landsat, NDWI, Water surface area.

Introduction:

Water bodies are among the important phenomena on the earth's surface in that studies and measurements can be made through remote sensing techniques and geographic information systems¹. Lakes act as basic components of the hydrological cycle and local ecosystems, and provide for human needs such as tourism, attractions, fishing, agricultural purposes, sources of freshwater and electric power generation. Changes in the lake area are highly sensitive to both climate change and human activities, spatial analysis techniques can help to estimate, and manage water², there is great importance in mapping lakes and accurately estimating their area changes because they contribute not only to understanding the significance of lake changes, but also the use and protection of lake water resources^{3,4}.

The most important factor affecting the water balance of lakes is the temperature, as the high temperature leads to an increase in evaporation

from the lakes and is accompanied by the scarcity and scarcity of sources for their regeneration, especially in dry and semi-arid regions characterized by high temperatures that lead to an increase in evaporation rates as is the case in the study area. An assessment of the water temperature in the lakes is essential to understanding their function and environmental condition. Additionally, LST is a proxy for analyzing water quality conditions and the impact of climate change on these systems. Although satellite-derived water temperature is a description of LST only in the upper layer (that is, about 100 meters upper, called "skin temperature"), it may provide important information about patterns of changes in water temperature in lakes, and it may be used in many studies, such as analysis of temperature patterns and heat balance, the spatial distribution of water quality variables, estimation of evaporation, spatial

gradients LSWT, temporal variation, LST patterns, and climate change over lakes^{5,6}.

Land surface temperature (LST) is an important biophysical parameter in surface energy processes and water balance at the regional level and global scales⁷, and is one of the most important switches in hydrology, meteorology, and surface energy balance⁸. It is one of the most important environmental criteria used to determine the exchange of energy and matter between the Earth's surface and lower atmosphere. LST is widely used to determine soil moisture content, to assess daily temperature change, to calculate surface long wave radiation to account for different types of evaporation^{9,10}.

An enormous number of studies present various calculations and techniques for LST recovery from Landsat, a portion of these calculations have likewise been applied in programming devices, for instance, there is a module for open source programming GIS. LST processes from Landsat 5, 7, and 8. Instruments like the ERDAS program have been created. Nonetheless, these instruments require programming establishment and, in particular, they require crude establishment satellite information downloads, which can be amazingly tedious^{11,12}.

Conventional strategies for estimating (field estimations) of lake water quality guarantee the ID of elements influencing the quality (Such as pollution by heavy metals, organic compounds, salinity...etc.), yet they are tedious and costly, or more everything, they don't give a spatial picture to help evaluation and observing of lake water quality. This issue was settled because of the simultaneous utilization of conventional field estimations and current far off detecting techniques, the last guides with the assortment of fast, transient and total information on water bodies and the execution of a spatial guide and fleeting evaluation of oceanic biological systems^{13,14}. Because of the absence of far off observing of lake water levels, remote sensing addresses a helpful and powerful option technique. Remote sensing data have been progressively used to screen and assess constant unique changes in enormous waterways inside dry grounds and can give valuable evaluations of the

lake's water balance just as yearly rates for water misfortune¹⁵. The utilization of remote sensing methods plans to see the elements of changes in height and surface space of water in lakes, which is a successful method to furnish data spatially and with high exactness^{16,17}. Calculating LST from remote sensing images is important because it illustrates most of Earth's physical, chemical, and biological processes¹⁸. There is a developing mindfulness among ecological researchers that remote sensing can and should assume a part in giving information important to evaluate the states of environments and change in them¹⁹. Remote sensing is an important way to follow in surface waters. It has the benefit that it tends to be applicable in relation to other direct estimates, and gives images of continuous cycles, yet it can also capture the temporal and spatial changes of surface waters.²⁰.

Hamrin Lake is a lake located in Diyala province, eastern Iraq. The lake follows the Hamrin Dam, which is located on the Alwand River in Diyala Governorate, which was inaugurated in June 1981 with the aim of protecting Diyala River Basin cities from seasonal floods. Hamrin Lake is located to the east of Saadia and is the strategic reservoir of water in Diyala²¹. The lake currently supplies more than 70% of Diyala regions with drinking and irrigation water.

The aim of the research is to assess the spatial and temporal differences of temperature and surface area in Lake Hamrin using Landsat 8 OLI / TIRS multi-spectral satellite images, and to know the extent of the ability of the NDWI to estimate the surface area of Lake Hamrin and compare it to the actual water level

Work Material and Methods:

Study area:

The study area was determined through field visits, using the GPS tool and with the help of Google Earth, as Hamrin Lake is located in Diyala Governorate, eastern Iraq, between latitudes 44° 53' 26.16" - 45° 07' 28.03" and 34° 04' 24.75" - 34° 19' 12.74". Fig. 1 shows the location of Lake Hamrin.

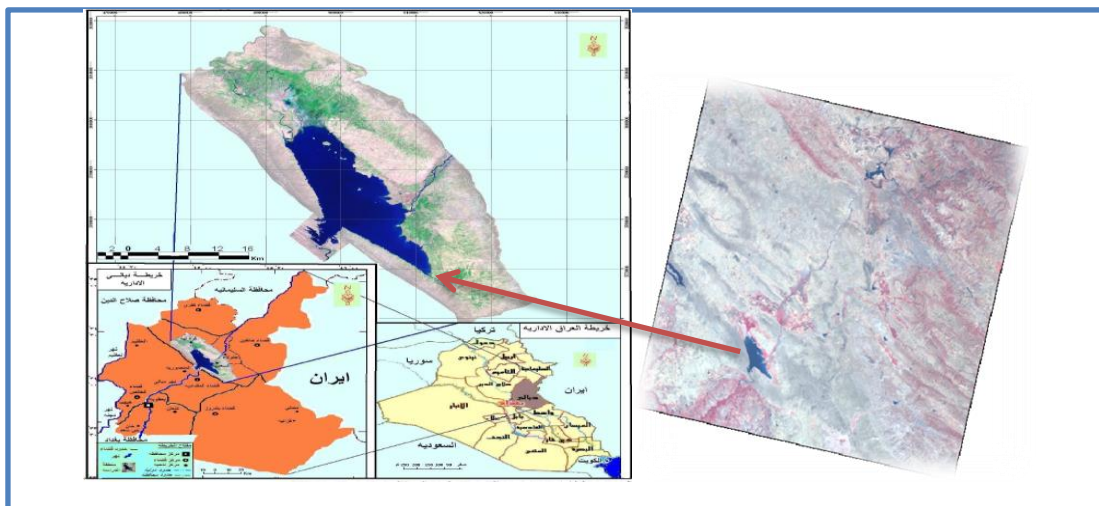


Figure 1. Location of Hamrin Lake in Diyala Governorate, Iraq, and Landsat satellite image

Satellite images:

The satellite images of the study area were used for the period from October 2019 to September 2020 (a water year), which amounted to 12 images (for band 10 and 11) of the Landsat 8 multi-spectral satellite, at an average of one image per month of the study period, as shown in Table 1

Table 1. Satellite data used in the study

No	satellite	Capture time	Path/row
1	Landsat 8	15/10/2019	168/036
2	Landsat 8	16/11/2019	168/036
3	Landsat 8	18/12/2019	168/036
4	Landsat 8	3/1/2020	168/036
5	Landsat 8	4/2/2020	168/036
6	Landsat 8	23/3/2020	168/036
7	Landsat 8	8/4/2020	168/036
8	Landsat 8	10/5/2020	168/036
9	Landsat 8	11/6/2020	168/036
10	Landsat 8	13/7/2020	168/036
11	Landsat 8	14/8/2020	168/036
12	Landsat 8	15/9/2020	168/036

Spectral indices utilized in the study: “Normalized Differences Water Index (NDWI)”

Table 2: NDWI statistical measures for Hamrin Lake and for each month

The month	Min	Max.	Mean	Std dev.
October-2019	-0.33881	0.28715	0.18241	0.02809
November-2019	-0.30296	0.25538	0.17129	0.02886
December-2019	-0.27514	0.23223	0.15261	0.02892
January-2020	-0.23962	0.19513	0.12872	0.02054
February-2020	-0.32331	0.25785	0.17945	0.03761
March-2020	-0.45862	0.30232	0.24137	0.04478
April-2020	-0.34972	0.23622	0.11196	0.07593
May-2020	-0.35414	0.34666	0.27174	0.06824
June-2020	-0.39761	0.28983	0.19931	0.04651
July-2020	-0.45789	0.32931	0.21631	0.05514
August-2020	-0.44274	0.32941	0.22529	0.04946
September-2020	-0.41950	0.27705	0.18745	0.05238

The reflectivity of water is high in the green frequency (0.52-0.60) μm and very little in the close to infrared frequency range (0.76-0.90) μm . The high reflectivity of the plant and soil in the infrared frequency range makes the NDWI esteems positive for water regions are thus enlightened and have positive qualities in NDWI when green and building regions seem dim and dark with negative or zero qualities⁽³⁾. The NDWI was calculated using the following equation²²:

$$\text{NDWI} = \frac{\text{Band}(\text{GREEN}) - \text{Band}(\text{NIR})}{\text{Band}(\text{GREEN}) + \text{Band}(\text{NIR})} \dots 1$$

Where Band(GREEN)= The third band of the Landsat 8(0.53–0.59) micrometer, Band (NIR)= The fifth band of the Landsat 8(Near Infrared 0.85–0.88) micrometer.

The surface area of the lake was calculated from each satellite image based on NDWI, which made it easy to determine and extract the outer limits of the lake water, and to draw the water body for it using ArcMap 10.8. Table. 2 shows the statistical measures of the NDWI for the lake and for each month, the numbers and statistical measures in table were calculated in the ArcMap 10.8 program.

“Normalized Difference Vegetation Index (NDVI)”:

It is quite possible that most notable unearthy and plant indices are utilized in the investigation of vegetation. It has been utilized widely in the investigation of worldly and spatial and temporal elements of vegetation cover. The NDVI record depends on the unearthy qualities of vegetation, contrasted with sans vegetation regions. Red strongly absorbs and reflects infrared rays. This is caused by the chlorophyll found in green leaves. Thus, areas with dense vegetation cover their horrific properties in the infrared, and areas with less thicker vegetation or devoid of vegetation. The NDVI profile is selected based on the discrimination in the measurement of radiation reflected in the closure by the red channels and the infrared channels divided by the amount of appearance in the two channels. “The value of the NDVI index is between -1 and + 1, the value of which is close to 1 (0.8-0.3) when there is dense vegetation, about 0.1 in the case of bare soil, and 0.2 – 0.3 with shrubs and grasses. The negative values of the guide are recorded in the case of clouds and snowcapped areas”²³. Its equivalent²⁴:

$$\text{NDVI} = \frac{\text{Band}(\text{NIR}) - \text{Band}(\text{Red})}{\text{Band}(\text{NIR}) + \text{Band}(\text{Red})} \dots 2$$

Where Band(NIR) = The fifth band of the Landsat 8 (Near Infrared 0.85–0.88) micrometer, Band(Red) = The second band of the Landsat 8 (0.64–0.67) micrometer.

index NDVI was used in the LST calculation of the lake and for each month using Erdas Imagine 2015 software.

Calculation of LST from satellite images:

At first, the Geometric and Radiometric remedy and Enhancement measures for the satellite data utilized in the examination were performed utilizing the Erdas Imagine 2015 program, depending on the two thermal bands B10 and B11 from each satellite image. The surface temperature of the lake water was calculated during the study period and as follows:

1- The numerical values of DN of each pixel in the image for the two thermal bands were converted to

the values of DN to Radiance using the following equation²⁵:

$$L\lambda = ML * Q_{cal} + AL \dots 3$$

where $L\lambda$ = radiative reflection ($m^2 * sr * m$), ML = is Standardization factor specific to each package, Q_{cal} = The numeric value of the pixel, AL = Correction factor

2- The temperature was calculated at the satellite TOA (Top of Atmospheric brightness highest temperature) Utilizing the following equation²⁶:

$$TB = (K_2 / (\ln(K_1 / L\lambda + 1))) \dots 4$$

Where: TB = The temperature on the satellite, K_1 = Conversion factor constant (Thermal band number), K_2 = Transformation factor steady (thermal band number).

Then the temperature values were converted from the Absolute temperature to the Celsius temperature using the following relationship²⁵.

$$C^\circ = K - 273.15 \dots 5$$

3- The percentage of vegetation cover is calculated according to the following equation²⁶:

$$Pv = \frac{NDVI - NDVI_{min}}{NDVI_{max} - NDVI_{min}} \dots 6$$

Where: $NDVI_{min}$ It is the lowest value of 0.2 NDVI for soil exposed pixels and $NDVI_{max}$ It is the highest value of NDVI 0.5 for a healthy vegetable pixel, Pv = The percentage of vegetation cover

4- The surface temperature was calculated using the following equation²⁵:

$$LST = TB / (1 + (L * TB / P) * \ln(e)) \dots 7$$

Where LST = Land Surface Temperature, P = (14380) Fixed value, $e = 0.004 * Pv + 0.986$ The emission correction factor is a constant value

5- The above calculations were made for bands 10 and 11 of each image, and then the average was taken from them, and thus the surface temperature of Lake Hamrin was extracted^{27,28}.

Results and Discussion:

In this study, the NDWI index was adopted in determining the water body of Lake Hamrin and its area in each image, as shown in Figs. 2, 3 and 4.

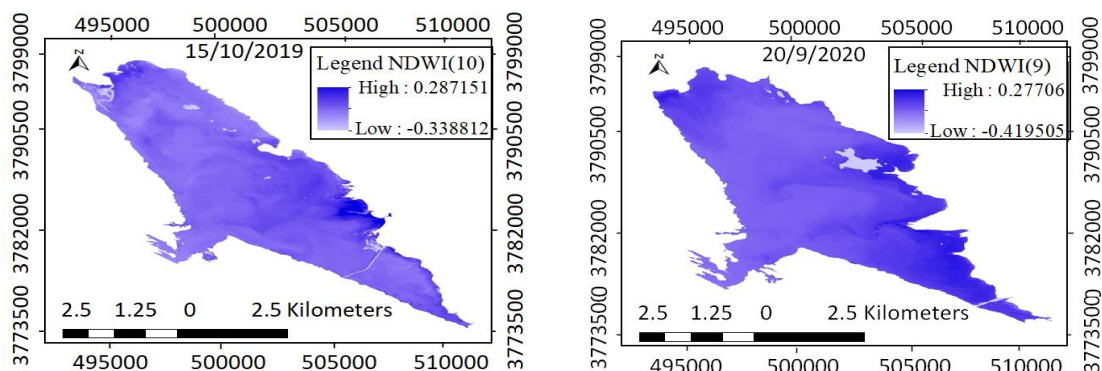


Figure 2. Deduction of the water body of Lake Hamrin, based on the NDWI(left surface area for October and the right surface area for September)

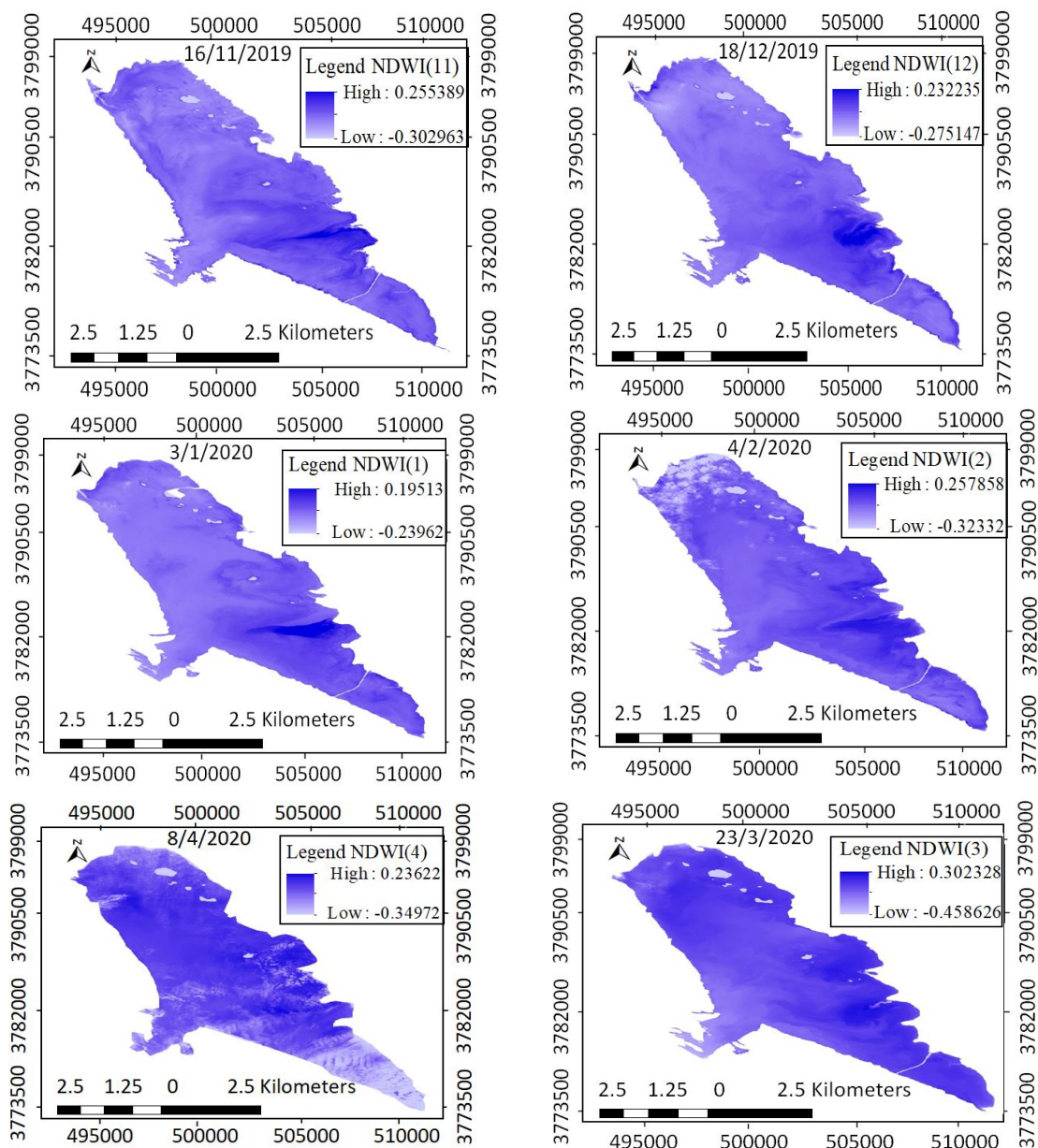


Figure 3. Deduction of the water body of Lake Hamrin, based on the NDWI (for months 11,12-2019 and 1,2,3,4-2020).

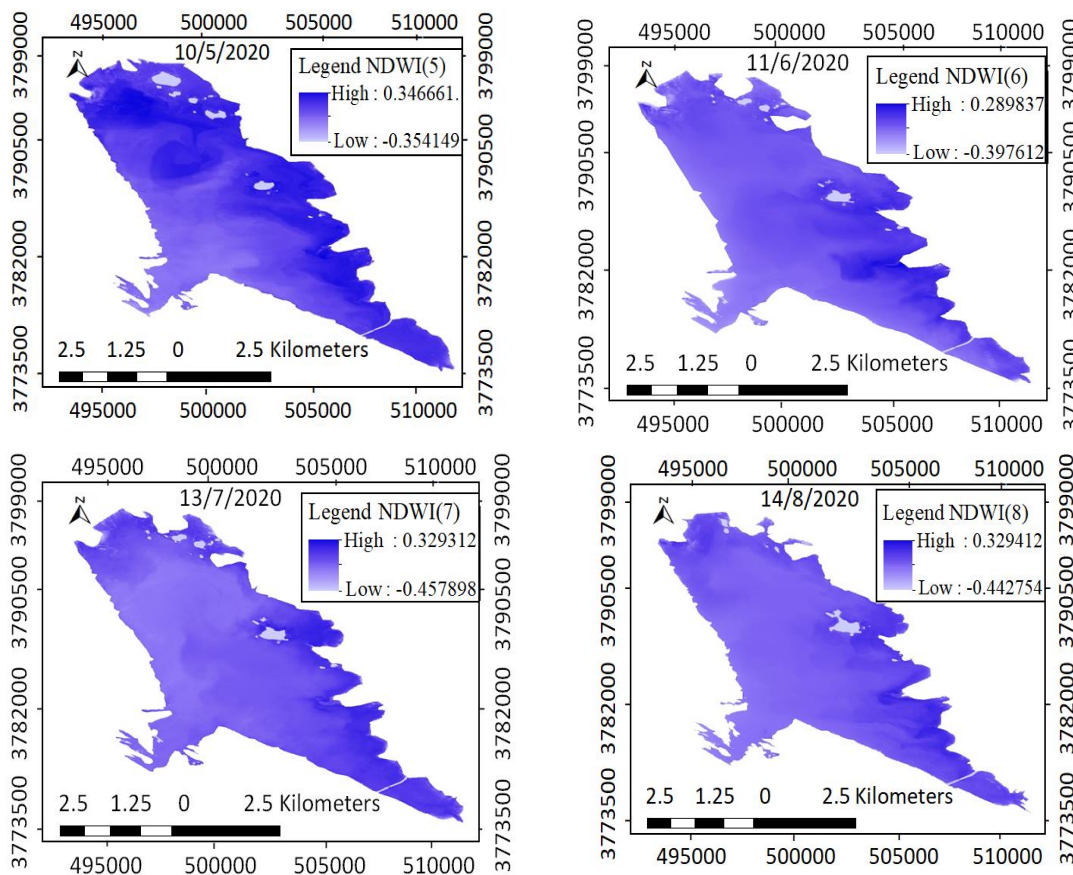


Figure 4. Deduction of the water body of Lake Hamrin, based on the NDWI (for months 5,6,7,8-2020)

Table. 3 shows the area of the lake calculated from the satellite images and the height of the water level inside the lake with the date of

taking each image, as these levels were obtained from official departments.

Table 3. Surface areas and water levels of Lake Hamrin from October-2019 to September-2020

The month	Area computed from satellite images (km ²)	The lake mean level (m)	Date
October-2019	264.617	102.173	15/10/2019
November-2019	232.595	100.851	16/11/2019
December-2019	226.802	100.403	18/12/2019
January-2020	206.558	100.214	3/1/2020
February-2020	212.774	100.276	4/2/2020
March-2020	200.519	99.982	23/3/2020
April-2020	196.512	99.301	8/4/2020
May-2020	174.833	98.722	10/5/2020
June-2020	159.535	98.398	11/6/2020
July-2020	154.562	98.225	13/7/2020
August-2020	152.186	97.872	14/8/2020
September-2020	140.202	97.333	15/9/2020

It is noted from Table 3 that the highest level 102.173 m and the largest surface area 264.617 km² for October are due to the heavy rains in the water year 2018-2019 preceding the water year 2019-2020, which led to the survival of the level and the surface area high but little. The rains for the study season and the continuation of water consumption in all fields led to a gradual decrease in the level and area until we reached the lowest

level 97.333 m and the lowest surface area 140.202 km² in September.

To extract the surface temperature of the lake from each spatial image and for each month of the study period (from the beginning of October 2019 until the month of September 2020) we used ArcMap 10.8 for this purpose, as in Figs. 5, 6 7, and Table 3.

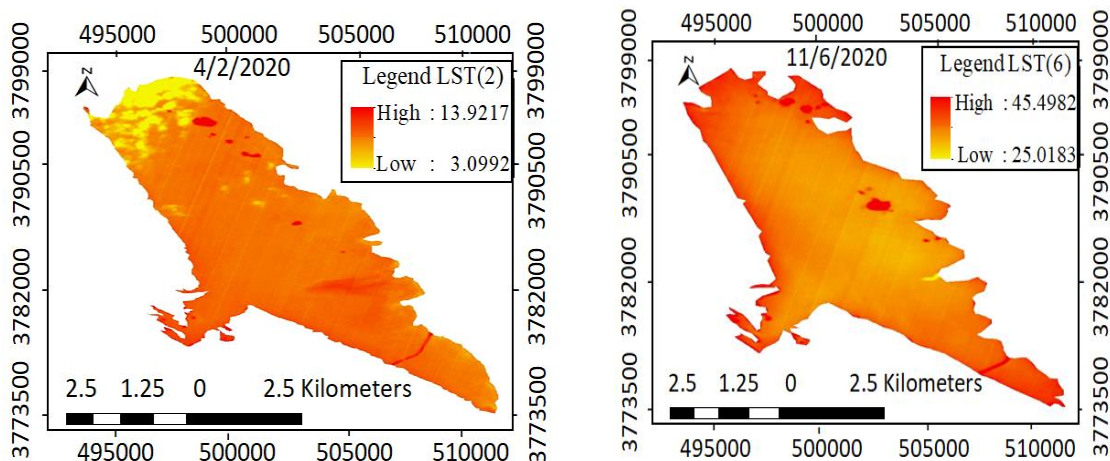


Figure 5. Monthly surface temperatures of Lake Hamrin (the lowest surface temperature was in February and highest in June).

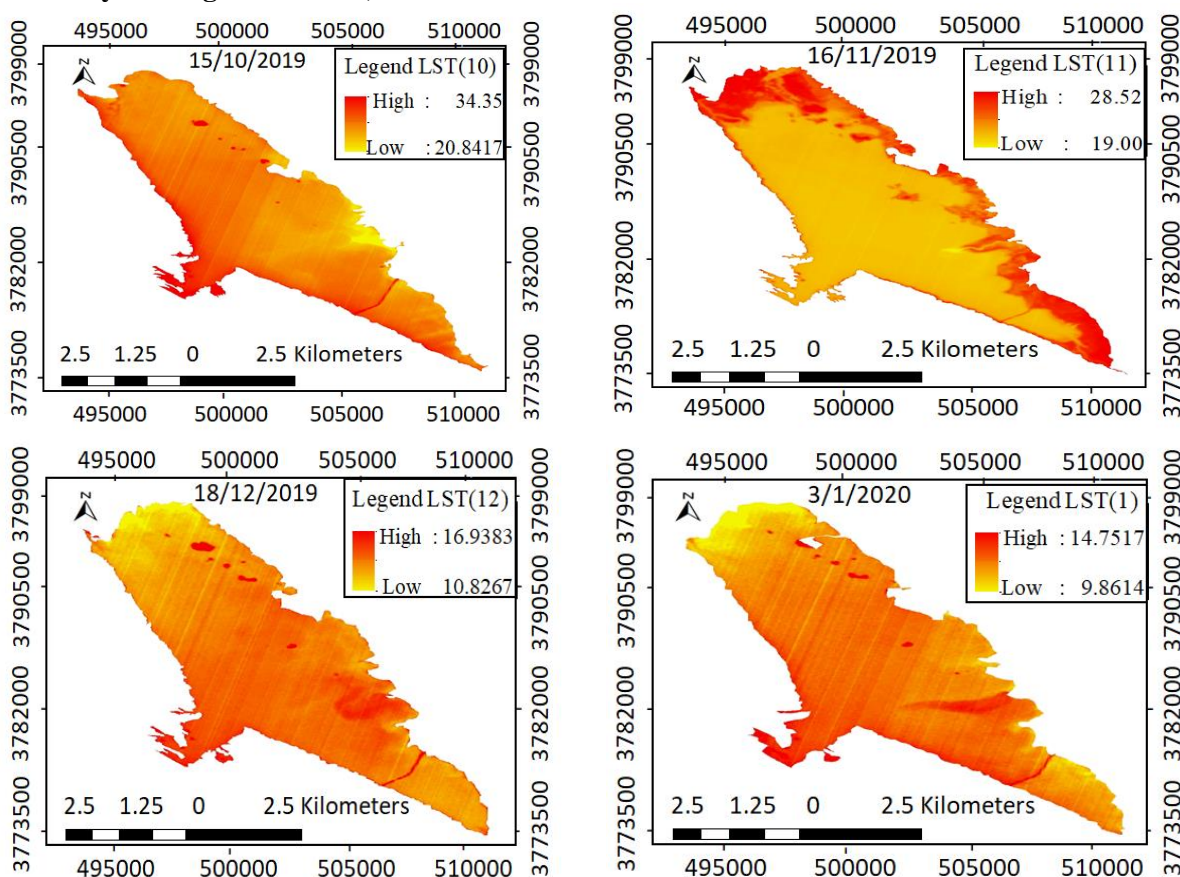


Figure 6. Monthly surface temperatures of Lake Hamrin (for months 10,11, 12-2019 and 1 -2020). Yellow represents the lowest temperature and red represents the highest temperature.

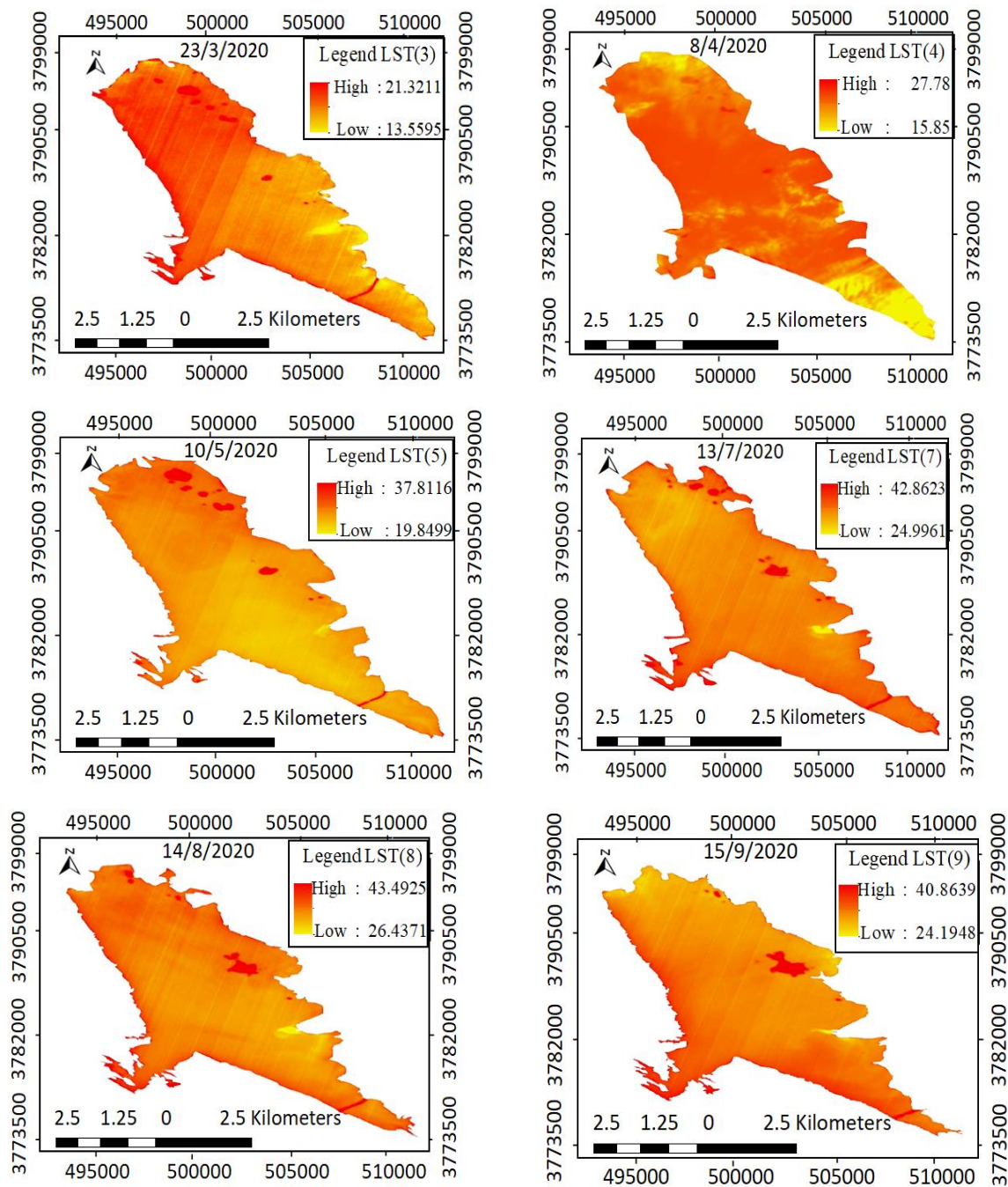


Figure 7. Monthly surface temperatures of Lake Hamrin (for months 3,4,5,7,8,9-2020)

Table 4. The monthly temperature values (°C) for Lake Hamrin for the period from October-2019 to September-2020, as inferred from satellite images.

The month	Min	Max.	Mean
October-2019	20.84	34.35	24.21
November-2019	19.00	28.52	20.64
December-2019	10.82	16.93	12.79
January-2020	9.86	14.75	11.25
February-2020	3.09	13.92	9.21
March-2020	13.55	21.32	15.12
April-2020	15.85	27.78	17.74
May-2020	19.84	37.81	22.08
June-2020	25.01	45.49	29.00
July-2020	24.99	42.86	28.97
August-2020	26.43	43.49	30.62
September-2020	24.19	40.86	27.55

It is noticed from Fig. 3 and Table. 4 that the temperature varies, as the temperatures at the edges of the lake are higher than the middle, due to the change in depth.

Conclusions:

The conclusion drawn from this study is there is change in the surface area and temperature of Lake Hamrin water throughout the year and is related to the seasons of the year and the rise and fall of the temperature, as the highest surface temperature reached in June 45.49 degrees Celsius due to the high temperatures for this month and the lowest in February 3.09 degrees Celsius, which is one of the months in which temperatures drop to the lowest level. The availability of rain that increases the surface area, and the consumption of lake water for various human activities leads to a decrease in the surface area, as it reached the highest surface area 264.617 km² for the month of October and the lowest surface area 140,202 km² for the month of September. The utilization of remote sensing and GIS innovations has helped a lot in checking changes, whether in surface area or temperature, which saves effort, time and cost. The results of this study put decision makers in taking the necessary precautions for the seasons of water scarcity and drought to meet the community's water needs in the areas of multiple human consumptions and at the same time take advantage of rainy seasons and water abundance and develop long-term strategic plans to maintain a sustainable water balance. The study recommends expanding the use of geospatial technologies to study the aquatic environment and follow-up the annual changes that occur in the surface area and temperature of Hamrin Lake, which helps decision makers to take the necessary measures to maintain water sustainability.

Author's declaration:

- Conflicts of Interest: None.
- I hereby confirm that all the Figures and Tables in the manuscript are mine. Besides, the Figures and images, which are not mine, have been given the permission for re-publication attached with the manuscript.
- Ethical Clearance: The project was approved by the local ethical committee in University of Diyala.

References:

1. Al-Qaisi KA. Calculating surface evaporation and change in the surface area of Lake Habbaniyah - Iraq using remote sensing and geographic information systems. M Sc. Thesis. College of Graduate Studies, Mutah University, Jordan, 2018; 1- 76.
2. Husam NM, Muwafaq AR, Bayan MH. Characterization of the Groundwater within Regional Aquifers and Suitability Assessment for Various Uses and Purposes-Western Iraq. *Baghdad Sci.J* .2021; 18(1), 670-686.
3. Abhijit S, Panhalkar S, Bansode S. Impact of land use land cover change on land surface temperature using geoinformatics techniques. *Int J Res Ana Rev*.2018; 5(4),550-559.
4. Aziz F, Kusratmoko E, Mandini D. Estimation of changes in the lake water level and area using remote sensing techniques (Case study: Lake Toba, North Sumatra). *IOP Conf. Series: Earth Environ Sci*. 561 2020; doi:10.1088/1755-1315/561/1/012022.
5. Javad A, Davood K, Esmaeil F, Khaled Z. Forecasting Surface Area Fluctuations of Urmia Lake by Image Processing Technique. *J Appl Res. water wastewater*. 2015; 2 (2),183-187.
6. Ruhakana A. The Estimation of Lake Naivasha Area Changes Using of Hydro-Geospatial Technologies. *Rwanda J Series*. 2016; 1(2), 144-157.
7. David P, Zina M, Nektrarios C, Michael A.2017. Online Global Land Surface Temperature Estimation from Landsat. *Remote Sens*. 2017; 9(12), 1208. <https://doi.org/10.3390/rs9121208>.
8. Garegin T, Vahagn M, Azatuhi H, Lilit M, Shushanik A. A Landsat 8 OLI Satellite Data-Based Assessment of Spatio-Temporal Variations of Lake Sevan Phytoplankton Biomass. *Geogr Ser*. 2017; 17(1), 83-89.
9. Xiangchen MJ, Shaohua Z, Sihan L, Yunjun Y. Estimating Land Surface Temperature from Landsat-8 Data using the NOAA JPSS Enterprise Algorithm. *Remote Sens*. 2019. 11(2). <https://doi.org/10.3390/rs11020155>.
10. Guha S, Govil H, Diwan P. Analytical study of seasonal variability in land surface temperature with normalized difference vegetation index, normalized difference water index, normalized difference built-up index, and normalized multiband drought index. *J Appl Remote Sens*. 2019; 13 (2), 24-38.
11. Himanshu G, Subhanil G, Anindita D, Neetu G. Seasonal evaluation of downscaled land surface temperature: A case study in a humid tropical city. *Heliyon*, 2019; 5(6), 123-1134.
12. Jimenez-Munoz JA, Sobrino D, Skokovic C, Cristóbal J. Land Surface Temperature Retrieval Methods from Landsat-8 Thermal Infrared Sensor Data. *IEEE Geosci. Remote Sens Lett*. 2014; 11(10), 1840-1843.
13. Yang K, Yu Z, Luo Y, Yang Y, Zhao L, Zhou X. Spatial and temporal variations in the relationship between lake water surface temperatures and water quality—A case study of Dianchi Lake. *Sci Total Environ*, 2017; 62(4), 859-871.
14. Lim J, Choi M. Assessment of water quality based on Landsat 8 operational land imager associated with human activities in Korea. *Environ Monit Assess*. 2015; 187, 384 <https://doi.org/10.1007/s10661-015-4616-1>.
15. Matheus H, Augusto F, David M, Lucia H. Comparison of Methods to Estimate Lake-Surface-

- Water Temperature Using Landsat 7 ETM+ and MODIS Imagery: Case Study of a Large Shallow Subtropical Lake in Southern Brazil. *Water*. 2018; 11(1), 168; 1-21, doi:10.3390/w11010168.
16. Mohamed A, Bastawesy b, Fikry I, Khalaf A, Sayed M. Arafat B. The use of remote sensing and GIS for the estimation of water loss from Tushka lakes, southwestern desert. *Egypt J Afr Earth Sci*. 2008; 52(3), 73-80.
 17. Duan SB, Li L, Tang BH, Wu H, Tan R. Generation of a time-consistent land surface temperature product from MODIS data. *Remote Sens Environ*. 2014; 140, 339-349.
 18. Arthur WS, Godfrey OM. Monitoring water depth, surface area and volume changes in Lake Victoria: integrating the bathymetry map and remote sensing data during 1993-2016. *Model Earth Syst Environ*. 2017; 3(2), 533-538.
 19. Osman O, Semih E, Filiz D. Use of Landsat Land Surface Temperature and Vegetation Indices for Monitoring Drought in the Salt Lake Basin Area. *Turkey Sci World J*. 2014; 14(1):55-71.
 20. Ugur A, Gordana J. Algorithm for Automated Mapping of Land Surface Temperature Using LANDSAT 8 Satellite Data. *J Sens*. 2016; 2,1-8.
 21. Ignacio F, Jose P, Floris O, Willem R. Comparison of Surface Water Volume Estimation Methodologies that Couple Surface Reflectance. *Water*. 2019; 11(4), 780. <https://doi.org/10.3390/w11040780>
 - 22.. Manikandan S. Assessment of surface water dynamics using multiplewater indices around adama woreda, Ethiopia. *ISPRS Annals of the Photogrammetry, Remote Sens Spat Inf. Sci*. 2018 4(5),181-188.
 23. Khalaf AB, Al-Jibouri A I J. Detection land cover changes of the Baquba city for the period 2014-2019 using spectral indices. *Iraq J Agric Sci*. 2020; 51(3), 805-815.
 24. Thomas P, Elias S. Assessing land degradation and desertification using vegetation index data: current frameworks and future directions. *Remote Sens*. 2014; 6, 9552-9575.
 25. Subhanil G, Himanshu G, Prabhat D. Analytical study of seasonal variability in land surface temperature with normalized difference vegetation index, normalized difference water index, normalized difference built-up index, and normalized multiband drought index. *J Appl Remote Sens*. 2019; 13(2),1-17.
 26. Sobrinoa J, Jimenez C, Leonardo P. Land surface temperature retrieval from Landsat TM 5. *Remote Sens. Environ*. 2004; 90(4), 434-440.
 27. Sun JJ, Xu YH. An ERDAS image processing method for retrieving LST and describing urban heat evolution: a case study in the Pearl River Delta Region in South China. *Environ Earth Sci*. 2009; 59(5), 1047-1055.
 28. Arthur WS, Godfrey OM. Monitoring water depth, surface area and volume changes in Lake Victoria: integrating the bathymetry map and remote sensing data during 1993-2016. *Model. Earth Syst Environ*. 2017; 3(2), 1-6.

استخدام التحسس النائي ونظم المعلومات الجغرافية لدراسة كشف التغير في درجة الحرارة والمساحة السطحية بحيرة حميرين

احمد بهجت خلف

قسم علوم التربة والموارد المائية، كلية الزراعة، جامعة ديالى، ديالى، العراق

الخلاصة:

اجريت هذه الدراسة على بحيرة حميرين الواقعة في محافظة ديالى وسط العراق بين خطي $44^{\circ} 53' 26.16''$ - $45^{\circ} 07' 28.03''$ ودائرتي عرض $34^{\circ} 04' 24.75''$ - $34^{\circ} 19' 12.74''$. اذ تمت في هذه الدراسة حساب المساحة السطحية لبحيرة حميرين من الصور الفضائية خلال الفترة الممتدة من شهر تشرين الأول 2019 الى ايلول 2020 وبمعدل صورة فضائية لكل شهر وباستخدام دليل اختلاف المياه الطبيعي NDWI فكانت اكبر مساحة سطحية 264.617 كم² لشهر اكتوبر واقل مساحة سطحية 140.202 كم² لشهر ايلول. وتم ايضا حساب درجة الحرارة السطحية لمياه البحيرة من الصور الفضائية للقمر الصناعي لاندسات 8 بالاعتماد على الحزم 10 (الأشعة تحت الحمراء الحرارية 1) و11 (الأشعة تحت الحمراء الحرارية 2) التي تتحسس الاشعة الحرارية، حيث بلغت أعلى درجة حرارة سطح في حزيران 45.95 درجة مئوية. بسبب ارتفاع درجات الحرارة لهذا الشهر وأدى مستوى لها في شيايط 3.09 درجة مئوية، وهو أحد الأشهر التي تنخفض فيها درجات الحرارة إلى أدنى مستوى لها. ساعد استخدام الاستشعار عن بعد وابتكارات نظم المعلومات الجغرافية كثيراً في التحقق من التغييرات، سواء في مساحة السطح أو درجة الحرارة، مما يوفر الجهد والوقت والتكلفة. وضعت نتائج هذه الدراسة متخذة القرار في اتخاذ الاحتياطات اللازمة لموسمي ندرة المياه والجفاف لتلبية احتياجات المجتمع المائية في مناطق الاستهلاك البشري المتعددة وفي نفس الوقت الاستفادة من مواسم الأمطار ووفرة المياه وتطوير خطط استراتيجية طويلة الأمد لأجل الحفاظ على توازن مائي مستدام.

الكلمات المفتاحية: التغير المناخي، درجة الحرارة لسطح الارض، لاندسات، NDWI، المساحة السطحية للمياه.